Asian Journal of Chemistry; Vol. 30, No. 7 (2018), 1608-1612

ASIAN JOURNAL OF CHEMISTRY

https://doi.org/10.14233/ajchem.2018.21291

Synthesis, Spectral, Structural and Antimicrobial Studies of Silver Nanoparticles and Ag(I) Complex of 2-Mercaptobenzothiazole

ALYA'A JABAR AHMED[1,*] and ABDULKAREEM MOHAMMED ALI ALSAMMARRAIE[2]

[1]Directorate of Scholarships and Cultural Relations, Ministry of Higher Education and Scientific Research, Baghdad, Iraq
[2]Department of Chemistry, College of Science, University of Baghdad, Baghdad, Iraq

*Corresponding author: E-mail: alyaa.jabbar@yahoo.com

Received: 16 February 2018; *Accepted*: 6 April 2018; *Published online*: 31 May 2018; AJC-18940

In the present study, Ag(I) complex is synthesized by reacting silver nitrate with ligand (2-mercaptobenzothiazole) in a 1:2 mole ratio. Furthermore, silver nanoparticles were prepared by the reduction of $AgNO_3$ using 2-mercaptobenzothiazole in dilute aqueous sodium citrate buffer solution. The Ag(I) complex are characterized by elemental analyses, flame atomic absorption, thermogravimetric analyses, molar conductance and magnetic susceptibility, UV-visible as well as FTIR spectroscopy. Analyses, linear geometry is suggested for the Ag(I) complex. The prepared nanoparticles are characterized using X-ray diffraction, scanning electron microscopy, energy dispersive microscopy, atomic force microscopy, vibrational and electronic spectroscopy. X-ray diffraction analysis revealed that silver nanoparticles with fcc crystal structure. The SEM micrographs indicated that the morphology is nearly rods shaped structure with an average diameter of about 100 nm. Biological activities of the ligand and its Ag(I) complex and silver nanoparticles are tested against *Staphylococcus aureus*, *Escherichia coli* bacteria and *Candida albicans*, *Candida tropicalis* fungi. It was found that both Ag(I) complex and silver nanoparticles have antimicrobial activities.

Keywords: Silver nanoparticles, 2-Mecaptobenzothiazole, Biological activities.

INTRODUCTION

Organisms, for example, microbes, molds, yeasts and viruses, in living condition are frequently pathogenic and cause serious diseases in individuals. The irresistible sicknesses treatment is a standout amongst the most imperative and testing issues as a result of the expanding number of safe microbial pathogens [1]. In this manner, there is a pressing requirement for creating or finding another successful antimicrobial specialists from natural and inorganic substances [2]. Silver ion and its compounds are highly toxic to microorganisms exhibiting strong biocidal effects on many species of bacteria but have a low perniciousness towards brute cells [3,4] .

The silver(I) complex plays an important role as carrier for the silver(I) ion to the biological system [5,6]. Antimicrobial nanoparticles basically comprise of metal, metal oxide and numerous biologically derived materials [7]. Its antimicrobial action is related with the characteristic structure of nanoparticles [8].The successful antimicrobial properties of these materials are for the most part due to their nanosize giving them interesting chemical and physical properties, for example, increased surface to volume ratio and high reactivity [8]. More recently, silver nanoparticles are started to be commonly used in the antimicrobial field for taking care of virus types of microbes such as fungi, virus and bacteria [9]. The silver nanoparticales (AgNPs) are very powerful tool that have many positive applications include in vitro use, used as biosensor materials. Furthermore, silver nanoparticles show to be a positive to enhance wound healing if AgNPs are used correctly in the medical industry due to their antibacterial, antifungal, antiviral, antiinflammatory and osteoinductive effect [10].

The research aims to synthesize and characterize a novel Ag(I) complex of 2-mercaptobenzothiazole and use the ligand as a reducing agent to synthesize silver nanoparticles. It highly predicted to become the useful tool to fight against microbial infections in the near future.

EXPERIMENTAL

All the solvents, starting materials as well as reagents were purchased commercially and then used without any further purification. The elemental analysis were carried out on a Fison EA 1108 analyzer, Fourier transform infrared analyzed spectra in the frequency range (4000-400 cm^{-1}) were recorded as KBr discs on FTIR 8300 Shimadzu spectrophotometer. Ultra-violet spectrophotometer in the range (200-1000) on Shimadzu UV-Vis 160 Shimadzu 680cc-flame was used to obtained the atomic

absorption measurements of the prepared complex .The values of magnetic susceptibility were obtained at room temperature using Magnetic Susceptibility Balance Bruke Magnet B.M. [6]. Conductivity measurements were carried out by WTW conductivity meter . The lattice parameters and crystal structure of the synthesized of silver nanoparticles were estimated by using Philips X-ray diffractometer (XRD-6000). Scanning electron microscopy (SEM) morphology of the prepared nanoparticles were estimated using an Oxford instrument attached to JSM-5300 scanning microscope equipment. The energy dispersive X-ray spectroscopy (EDS) analysis was used to determine the elemental analysis of particles.

Synthesis of Ag(I) complexes: A solution of $AgNO_3$ (5 mmol) dissolved in 50 mL of absolute ethanol was added gradually drop by drop to of ligand (10 mmol) dissolved in 80 mL of absolute ethanol. The mixture was stirred for 15 min and the resulted precipitate was filtered off washed with distilled water and then dried under vacuum machine. Elemental analysis for 2-mercaptobenzothiazole: Found (calcd.) %: C 51.99 (50.22); H 2.76 (2.98); N 8.40 (8.37); S 39.05 (38.26), where the elemental analysis for Ag(I) complex as: Calcd. (found) %: C 30.75 (31.02); H 1.53 (1.63); N 5.06 (5.11); S 24.62 (24.85); Ag 24.62 (24.85).

Synthesis of silver nanoparticles: Silver nitrate (4 mL, 0.59 mmol) solution was mixed with 2-mercaptobenzothiazole (0.89 mmol) and then dissolved in 4 mL of absolute ethanol at room temperature. A freshly prepared dilute aqueous sodium citrate buffer solution (1 %) was added steadily while the mixture was being vigorously stirred. There was an immediate colour change of this solution from colourless to brown indicates the formation of silver nanoparticles which can be obtaind by filtration then washed with ethyl alcohol to remove excess capping agent.

Antimicrobial activity: The antibacterial activity of the synthesized compound was tested against *Escherichia coli* and *Staphylococcus aureus* bacteria and *Candida albicans*, *Candida tropicalis* fungi. Each compound was freshly synthesized by dissolving in DMSO in order to obtain a final concentration of 200 µg/mL. The antibacterial test was performed according to disc diffusion method [11]. Generally, in the typical procedure, the wall was made on agar medium inoculated (1 mL/100 mL of medium) with the microorganism. The wall diffusion was filled with the test solution using micropipette and the plate was preincubated for 1 h at room temperature and incubated at 35 ºC for 24 h.

RESULTS AND DISCUSSION

Electronic spectra: The ultraviolet visible spectrum of 2-mercaptobenzothiazole and its Ag(I) complex in methanol solvent is shown in Fig. 1 and 2. The spectrum of 2-mercaptobenzothiazole exhibited two bands at the wavelength (43478 and 30395 cm^{-1}). The band at 43478 cm^{-1} due to the intra-ligand ($n\rightarrow\pi^*$) transition located on C=C and C=N which are in conjugated with the aromatic nucleus (benzothiazole ring). The second absorption band (30395 cm^{-1}) attributed to ($n\rightarrow\pi^*$) transition within C=N group (Fig. 1). The UV-visible spectrum of the present dark yellow Ag(I) complex exhibited three bands at (48543, 43668 and 44843 cm^{-1}) (Fig. 2). These bands are the resultant of metal-ligand charge transfer (M→LCT) or ligand-centered ($\pi\rightarrow\pi^*$) transition, metal-metal interaction [12].

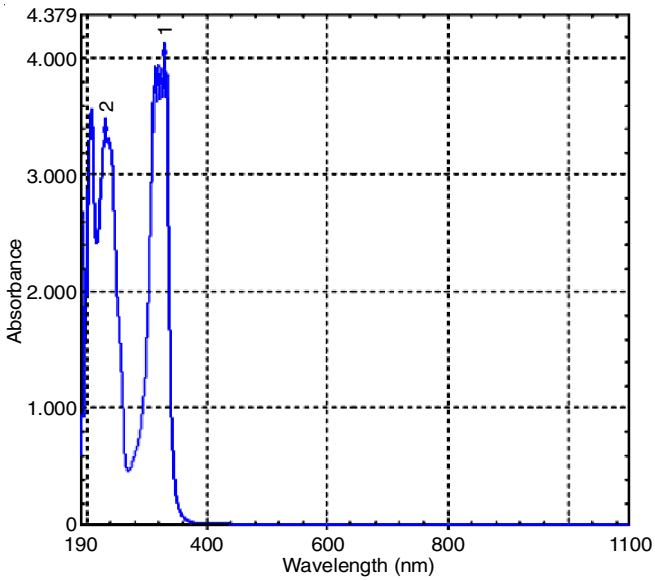

Fig. 1. Electronic spectra of 2-mercaptobenzothiazole

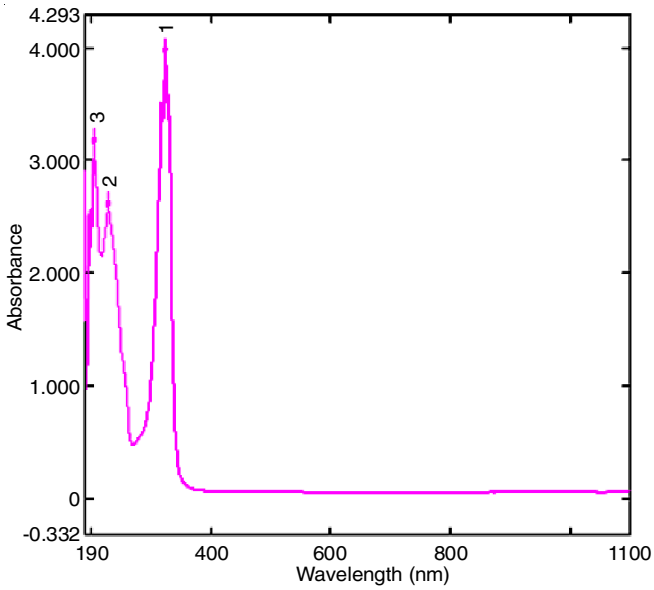

Fig. 2. Electronic spectra of Ag(2-mercaptobenzothiazole) complex

FT-IR analysis: FT-IR spectra of ligand and its Ag(I) complex were recorded in KBr discs. The bands observed at 1456 cm^{-1} is assigned to C-N stretching vibrations. The weak bands observed at 2671 and 2505 cm^{-1} can be interpreted as overtone bands of the fundamental frequencies at 1321 and 1246 cm^{-1}. The band observed at 1597 cm^{-1} is assigned to C=C stretching mode. The symmetric out-of-plane C-H vibration was observed as a very strong band at 750 cm^{-1}. The weak bands at 607 cm^{-1} and the strong band observed at 667 cm^{-1} were assigned to C-S stretching mode. The spectrum of 2-mercabtobenzothiazole also displays four bands 1496, 1321, 1080 and 850 cm^{-1} assigned to thioamide bands [13], contains a thioamide group (HNC=S) and has contribution from δ(C-H) + δ(N-H), ν(C=S) + ν(C-H), ν(C-N) and ν(C-S), respectively. These thioamide bands II are shifted to higher wave numbers ,where the thioamides bands III and IV are strongly shifted to lower wave numbers in the spectra of the complex supporting sulfur donation and deprotonation of the ligand as well. Furthermore, the

(HNC=S) bands I are not affected by complexation. The spectrum of 2-mercaptobenzothiazole displays a medium strong band at 3113 cm^{-1} due to ν(NH). In the FT- IR spectra of Ag(I) complex, the band due to ν(N-H) are not found to be present. For this reason, someone should expect the charge balance in the complexes ought to be maintained. Accordingly, 2-mercaptobenzothiazole acts as a monobasic bidentate ligand coordinated to the metal ions through the deprotonated to thiocarbonyl sulphur and nitrogen atoms. This coordinate was supported by appearance ν(Ag-S) and ν(Ag-N) band in the region 434 and 523 cm^{-1}. A band observed at 3431-3419 cm^{-1} in the spectrum of Ag(I) complex, assigned to ν(-OH) which refers to the presence of uncoordinated water molecule.

Magnetic susceptibility and conductivity measurements: The magnetic properties of transition metal complexes coordination compound are due to unpaired electrons bearing in the partially filled *d*-orbital in the outer shell of these elements [14]. The complex dimagnetic moment in solid state is breakthrough to be zero Niels Bohr magneton and Ag (I) metal moiety exhibited linear geometry. The measurements of molar conductivity indicated that the complex is electrolyte.

Thermal analysis: Thermogravimetric (TG) curve of the complex in the 25-600 ºC range under N_2 are shown in Fig. 3. The TG curve of $[AgL_2]\cdot H_2O\cdot NO_3$ shows one stages of decomposition within the temperature (221.9 ºC), where a water molecule (found: 2.7 mg; calcd.: 2.6 mg) was lost. The results obtained in this study are in agreement with the structures suggested from the analytical data.

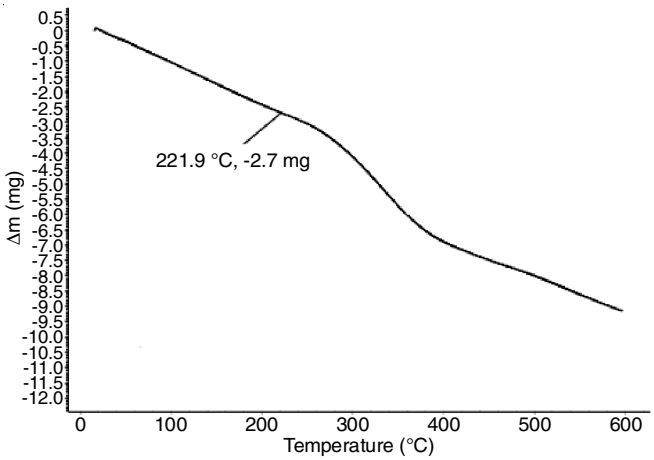

Fig. 3. Thermogravimetric curve of $[AgL_2]\cdot H_2O\cdot NO_3$

Characterization of silver nanoparticles

Structural studies: The X-ray diffraction pattern of the synthesis silver nanoparticles is shown in Fig. 4. The peaks observed at 2θ value 31.16º, 44.7º, 68.5º, 77º which can be indexed to the (111), (200), (220), (311) characteristic reflection plane. This observation indicates the formation of metallic Ag with face-centered cubic structure additionally, the existence of some traces of silver oxide is found and the reason behind that might be relevant to oxidation of silver nanoparticles after being exposed to air [15]. Similar characteristic peaks and corresponding reflection planes are reported earlier [2,16]. The crystalline size of silver nanoparticles is calculated from X-ray line broadening using Debye-Scherrer equation [17]:

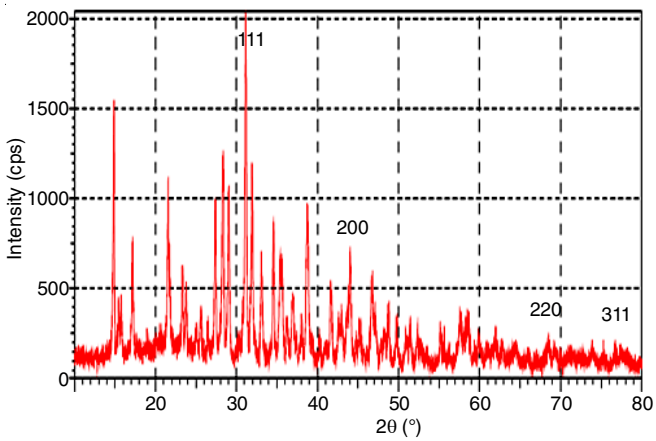

Fig. 4. X-ray diffraction of silver nanoparticles

$$D = \frac{k\lambda}{\beta\cos\theta} \quad (1)$$

where λ = X-ray wavelength (CuK_α radiation equals to 1.54 Å); θ = Bragg diffraction angle; β = FWHM of XRD peak appeared at the diffraction angle θ. The size of the particles is found to be 41 nm.

Scanning electron microscopy analysis: The size and morphology of the prepared silver nanoparticles were investigated by scanning electron microscopy. Fig. 5(a-c) shows the SEM images of silver nanoparticles. It can be clearly seen from these images that a common characteristic of the particles is rods shape. It is also shown that particles are mutually different in sizes about 100 nm.

The grain size as calculated by XRD and SEM are quite different. In XRD, the grain size is measured by the extended to the crystalline region that diffracted X-rays coherently, whereas, in SEM the measurement is obtained by the difference between visible grain boundaries. Hence, the XRD measurements produce smaller peaks.

The elemental composition of the silver nanoparticles is analyzed by energy dispersive X-ray spectroscopic analysis. In the left part of EDS spectrum recorded clearly shows three peaks located in 3 kV (Fig. 6). Those maxima are directly attributed to the silver characteristic lines. The maximum located on part of spectrum at 0.2 kV is connected with oxygen characteristic line. The spectra obtained during EDS studies are used for carrying out the quantitative analysis. Quantitative analysis proved high silver contents (65.61 %) in the examined samples. Except for silver, it also showed the presence of oxygen, which is amounted to be 34.39 %.

Spectroscopic studies: The UV-visible spectrum of silver nanoparticles is shown in Fig. 7. Silver nanostructures show SPR depending on different shapes and sizes at various frequencies. The prepared silver nanoparticles showed an absorption band due to absorption of visible light along both the width of the nanorods The weak peak at 300 nm belongs to the optical signatures of silver nanorods, whereas the broad absorption peak at 420 nm is assigned to the oscillation of conduction band electrons as the surface plasmon resonance. The broad absorption band observed in UV-visible spectrum display that the final product should be the presence of both silver nanorods and dispersive particles. Moreover, it is in agreement with

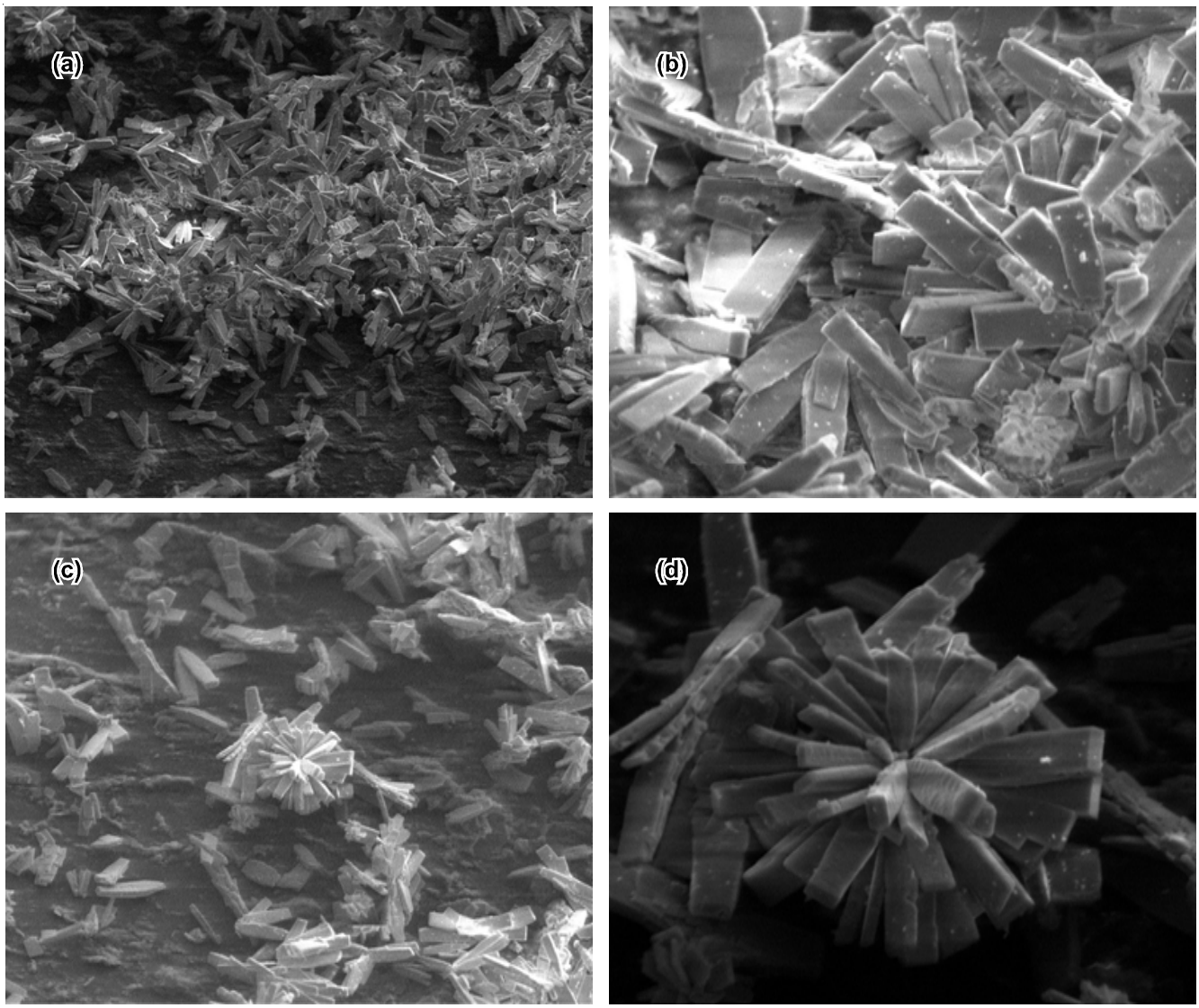

Fig. 5. Scanning electron microscope image of silver nanoparticles

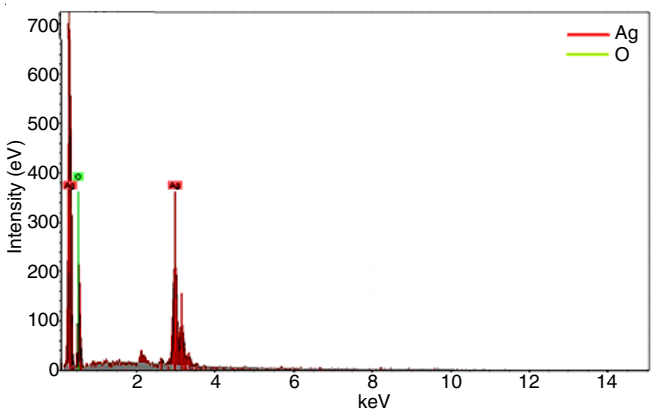

Fig. 6. SEM-EDS spectra of silver nanoparticles

previous studies [18] as shown in Fig. 7. The band gap energies are calculated using the following equation:

$$E_g = \frac{1240}{\lambda_{max}} \quad (2)$$

where E_g is the band gap energy, the value of 1240 is the hc (photon energy) and λ_{max} is the wavelength in nanometer. The

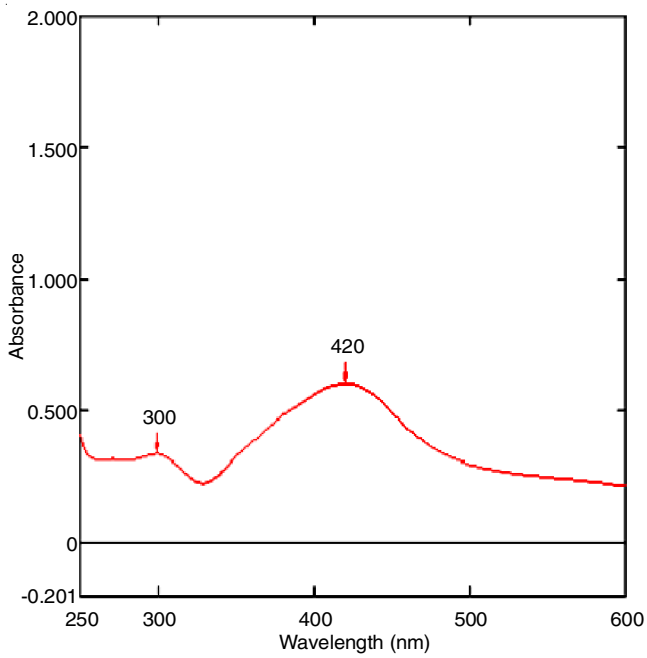

Fig. 7. Electronic spectra of the synthesis silver nanoparticles

calculated values the band gap energies are 3.7 eV (329 nm) and 2.9 eV (420 nm) for 2-mercaptobenzothiazole and silver capped 2-mercaptobenzothiazole, respectively. These values are obviously decreased after doping, this indicates the optical properties depends on the short range order in the defects state as well as amorphous state associated with it, decrease in the band gap energies in the present system might return to the reduction in disorder of the system and increasing in the density of defect states. So, it can be concluded that the optical properties of 2-mercaptobenzothiazole effected by silver nanoparticles doping.

The interaction of silver nanoparticles obtained with 2-mercaptobenzothiazole is confirmed by FT-IR spectra. Infrared studies are employed to achieve the purity and nature of silver nanoparticles. The bands obtained are compared with ligand and however less intense peaks with slight shift are observed in the silver nanoparticles. The results showed some differences between the spectra of 2-mercaptobenzothiazole and it capped silver nanoparticles due to thioamide on silver nanoparticles form is a close-packed layer and molecular motion is constrained. The ν(NH) band appeared at 3120 cm^{-1} which is absent in metal capped nan particles indicated the capping of metal with 2-mercaptobenzothiazole, giving strong evidence that 2-mercaptobenzimidazole anchors on silver surface through nitrogen atom in thiazole ring. The band appeared at (3460 cm^{-1}) attributed to O-H stretching and deformation I indicate the water adsorption on the metal surface.

Biological studies: The *in vitro* antibacterial efficiency of the synthesized silver nanoparticles and Ag(I) comples using 2-mercaptobenzothiazole as a ligand on selected bacteria *E. coli* and *S. aureus*, and *Candida albicans* and *Candida tropicalis* fungi is carried out. Comparing the biological activity of 2-mercaptobenzothiazole and its Ag(I) complex with silver nanoparticles, the values indicate that silver nanoparticles have higher antibacterial activity than free ligand and its Ag(I) complex (Table-1). This indication may be simply due to more prominent lipophilic nature of the complex with added effect of silver nanoparticles. Such increased action of the complexes can be clarified on the basis of Tweedy's chelation theory and Overtone's concept. On chelation, the polarity of the metal particle decreased to a more extant degree because of the overlap of ligand orbital and partial sharing of positive charge of metal ion with donor groups. Moreover, it increases the delocalization of π-electrons over the entire chelate ring and upgrades the lipophilicity of the complex. This expanded lipophilicity improves the entrance of the complex into lipid membrane and consequently obstructs the blocks the metal restricting locales on proteins of microorganisms [19].

TABLE-1
EVALUATION OF THE ANTIMICROBIAL ACTIVITY

Compound	Diameter of inhibition zone growth (mm/mg sample)			
	S. aureus	*E. coli*	*Candida albicans*	*Candida tropicalis*
2-MBT	8	12	13	–
Ag(I) complex	10	14	15	8
Ag nanoparticles	14	15	28	10

Conclusion

Silver nanoparticles were prepared by chemical reduction of silver nitrate using 2-mercaptobenzothiazole. The UV and FT-IR spectra confirmed the formation of silver nanoparticles. The rods shapes structures of the nanoparticles were observed in SEM with particle sizes about 100 nm. The prepared silver nanoparticles have antibacterial effect on the bacteria *E. coli* and *S. aureus*, and *Candida albicans*, *Candida tropicalis* fungi. On the other hand, Ag(I) complex prepared from the same ligand exhibited considerable antibacterial and antifungal activities.

REFERENCES

1. A.A. Soayed, *Inorg. Chim. Acta*, **429**, 257 (2015); https://doi.org/10.1016/j.ica.2015.02.012.
2. P. Jeevan, K. Ramya and A.E. Rena, *Indian J. Biotechnol.*, **11**, 72 (2012).
3. A. Oloffs, C. Grosse-Siestrup, S. Bisson, M. Rinck, R. Rudolph and U. Gross, *Biomaterials*, **15**, 753 (1994); https://doi.org/10.1016/0142-9612(94)90028-0.
4. H. Oka, T. Tomioka, K. Tomita, A. Nishino and S. Ueda, *Met. Based Drugs*, **1**, 511 (1994); https://doi.org/10.1155/MBD.1994.511.
5. K. Nomiya, A. Yoshizawa, K. Tsukagoshi, N.C. Kasuga, S. Hirakawa and J. Watanabe, *J. Inorg. Biochem.*, **98**, 46 (2004); https://doi.org/10.1016/j.jinorgbio.2003.07.002.
6. M. Hanif, A. Saddiqa, S. Hasnain, S. Ahmad, G. Rabbani and A.A. Isab, *J. Spectrosc.*, **22**, 51 (2008); https://doi.org/10.1155/2008/170213.
7. Sh. Ranghar, P. Sirohi, P. Verma and V. Agarwal, *Braz. Arch. Biol. Technol.*, **57**, 209 (2013); https://doi.org/10.1590/S1516-89132013005000011.
8. J. Pulit, M. Banach, R. Szczyglowska and M. Bryk, *Acta Biochim. Pol.*, **60**, 795 (2013).
9. N. Beyth, Y. H.Haddad, A.Domb, W.Khanand and R. Hazan, *Evid. Based Complem. Altern. Med.*, **Article ID 246012** (2015); https://doi.org/10.1155/2015/246012.
10. P. Pandey and M. Dahiya, *J. Crit. Rev.*, **3**, 18 (2016).
11. M.G. Guzman, J. Dille and S. Godet, *Int. J. Chem. Biomol. Eng.*, **2**, 104 (2009).
12. P. Aslanidis, A.G. Hatzidimitriou, E.G. Andreadou, A.A. Pantazaki and N. Voulgarakis, *Mater. Sci. Eng. C*, **50**, 187 (2015); https://doi.org/10.1016/j.msec.2015.02.014.
13. S.S. Kandil, N.R. El-Brollosy and A. El-Dissouky, *Synth. React. Inorg. Metal-Org. Nano-Metal Chem.*, **30**, 979 (2000); https://doi.org/10.1080/00945710009351813.
14. E. Yousif, Y. Farina, Kh. Kasar, A. Graisa and K. Ayid, *Am. J. Appl. Sci.*, **6**, 582 (2009); https://doi.org/10.3844/ajassp.2009.582.585.
15. A. Shafaghat, *Synth. React. Inorg. Metal-Org. Nano-Metal Chem.*, **45**, 381 (2015); https://doi.org/10.1080/15533174.2013.819900.
16. C. Liu, X. Yang, H. Yuan, Z. Zhou and D. Xiao, *Sensors*, **7**, 708 (2007); https://doi.org/10.3390/s7050708.
17. K. Jyoti and A. Singh, *J. Genetic Eng. Biotechnol.*, **14**, 311 (2016); https://doi.org/10.1016/j.jgeb.2016.09.005.
18. N. Budhiraja, A. Sharma, S. Dahiya, R. Parmar and V. Vidyadharan, *Int. Lett. Chem. Phys. Astron.*, **19**, 80 (2013); https://doi.org/10.18052/www.scipress.com/ILCPA.19.80.
19. Sh. Sujarania, T. Sironmani and A. Ramu, *Dig. J. Nanomater. Biostruct.*, **7**, 1843 (2012).